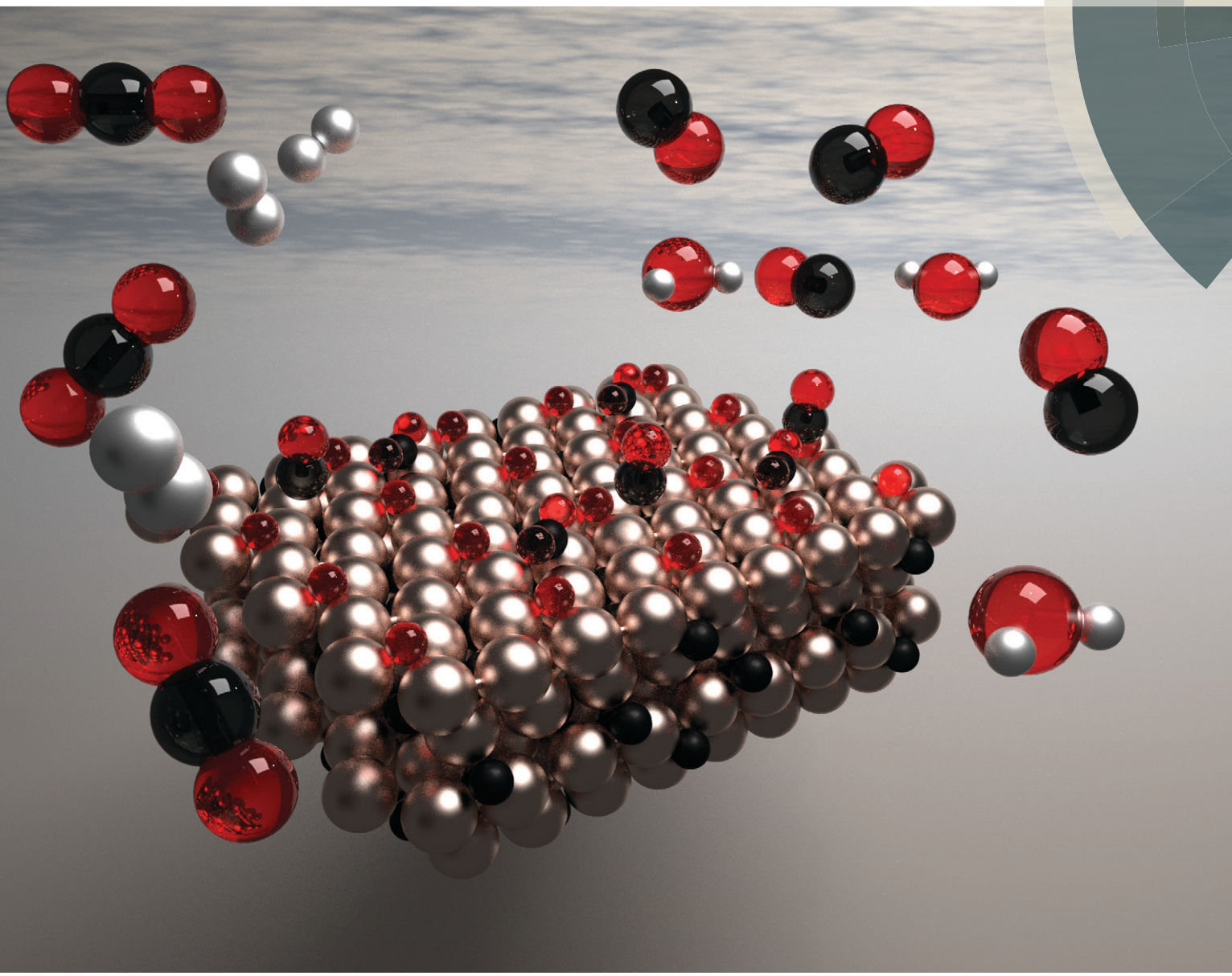


Catalysis Science & Technology

rsc.li/catalysis



ISSN 2044-4761



PAPER

Giannis Mpourmpakis *et al.*
Elucidating the role of oxygen coverage in CO_2 reduction on Mo_2C



Cite this: *Catal. Sci. Technol.*, 2017,
7, 5521

Elucidating the role of oxygen coverage in CO₂ reduction on Mo₂C†

Mudit Dixit, ‡^a Xi Peng, ‡^a Marc D. Porosoff,^b
Heather D. Willauer^c and Giannis Mpourmpakis *^a

Molybdenum carbide (Mo₂C) is a promising and low-cost catalyst for the conversion of CO₂ to CO. However, the underpinning mechanism occurring on the catalyst surface and the understanding of the catalyst structure under the reaction conditions is still elusive. In this study, we employ first principles calculations to understand the CO₂ dissociation mechanism on β-Mo₂C (001) under different oxygen coverage on the catalyst surface (oxycarbide). Our results demonstrate that with increasing oxygen coverage, there is an electronic modification on the catalyst surface (e.g. d-band shift on Mo atoms), that in turn, tunes the interactions of the adsorbates and the CO₂ dissociation barriers. Interestingly, we reveal linear relationships between the oxygen coverage and electronic modification with the reactivity of the catalyst. We show that CO₂ can adsorb and dissociate on the oxygen covered Mo₂C surface, even in the presence of surface oxygen up to 0.5 monolayer (ML). Our results rationalize a series of experimental observations.

Received 1st September 2017,
Accepted 9th October 2017

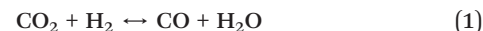
DOI: 10.1039/c7cy01810j

rsc.li/catalysis

Introduction

The atmospheric concentration of carbon dioxide (CO₂) has been dramatically increasing over the past century. As CO₂ is one of the major contributors to the greenhouse effect, several environmental concerns are associated with its excessive presence in the atmosphere.^{1–4} Solutions that are effective and efficient in removing CO₂ from the atmosphere are in urgent need.⁵ In spite of the environmental issues associated with CO₂, due to its low cost, abundance, nontoxicity, and nonflammable nature, CO₂ is an attractive renewable C₁ feedstock for the production of valuable chemicals, fuels, and materials.^{6–9}

The conversion of CO₂ is often limited by the high strength (192 kcal mol⁻¹) of the C=O bond.¹⁰ However, high energy materials such as hydrogen or organometallics are often capable of converting CO₂ to useful chemicals.⁸ One of the promising routes for CO₂ utilization is to convert CO₂ to carbon monoxide (CO) *via* the reverse water-gas shift reaction (RWGSR) (eqn (1)), which can then be used to obtain valuable hydrocarbons *via* Fischer-Tropsch synthesis (eqn (2)).^{9,11}



The traditional metal catalysts for the transformation of CO₂ such as Pt, Ru, and Pd, have limited use in industrial scale productions, due to their high cost.¹² Since CO₂ is a promising renewable C₁ feed for producing high-value chemicals,^{6,7} identifying new, low-cost catalysts that can effectively convert CO₂ are needed.

Transition metal carbides (TMCs) are promising catalysts, which display catalytic properties similar to noble metals (Pt and Pd).^{13–19} Among carbides, molybdenum carbide (Mo₂C) exhibits high activity for a wide range of catalytic reactions, such as water gas shift,^{20,21} steam reforming,²² hydrogenolysis of alkanes,²³ dehydrogenation of propane,²⁴ etc. Considering the high activity and relatively low cost of Mo₂C compared to traditional noble metal catalysts, the interaction of CO₂ with TMC surfaces is of marked interest.^{15,25,26} Porosoff *et al.* demonstrated that Mo₂C is an active catalyst for CO₂ conversion to CO, and showed that the active phase of the catalyst is an oxycarbide phase, using ambient-pressure X-ray photoelectron spectroscopy (XPS) and *in situ* X-ray absorption near edge spectroscopy (XANES).⁹

Previous studies established that electronic perturbation of the local environment by alkali metal promotion can enhance adsorption of apolar molecules and the activity of the catalyst. Mortensen *et al.* found that alkali metals promote N₂ dissociation over Ru catalysts.²⁷ Linic and Barteau showed that alkali metal (Cs) enhances the selectivity of ethylene

^a Department of Chemical Engineering, University of Pittsburgh, Pittsburgh, PA 15261, USA. E-mail: gmpourmp@pitt.edu

^b Department of Chemical Engineering, University of Rochester, Rochester, NY 14627, USA

^c Materials Science and Technology Division, Naval Research Laboratory, Washington DC, USA

† Electronic supplementary information (ESI) available. See DOI: 10.1039/c7cy01810j

‡ These authors contributed equally.

epoxidation over Ag (111), due to an introduced electric field.²⁸ In a recent study, Xin and Linic studied the O₂ dissociation over Ag (111) and demonstrated that the major contribution of alkali metal (Cs) promotion arises due to the interaction of the induced electric field with the static dipole moment of the oxygen-adsorbed surface.²⁹ Interestingly, alkali metal promoted Mo₂C-based catalysts showed superior activity compared to the clean catalysts.^{30–32} Solymosi *et al.* showed that K-promotion dramatically enhances the CO₂ adsorption behavior on the Mo₂C/Mo (111).³² Recently, in a combined experimental and computational study, it was shown that K-promoted Mo₂C was a selective RWGSR catalyst over a wide range of conversions and the catalytically active oxycarbide phase may be critical for the stability and selectivity of the catalyst.³³ Interestingly, using density functional theory (DFT) calculations, the authors noted a high exothermicity of the dissociated state of CO₂ (CO* + O*) on the metallic phase of Mo₂C, supporting the formation of oxycarbide phase.³³ These results clearly indicate that under experimental conditions, the metal carbide surface may be converted to an oxygenated metal-carbide surface. Notably, if surface hydroxyl groups are present under reverse water-gas shift reaction (RWGSR) conditions, these can produce HCO₃⁻ (bicarbonate) species as surface species.³⁴ Although the possibility of surface hydroxyl formation cannot be ruled out, experimentally, there was no evidence of surface hydroxyls. Yet, a fundamental understanding of the CO₂ conversion to CO under different oxygen coverage (and formation of oxycarbide phase) on Mo₂C is still elusive.

In this study, we employ DFT calculations to investigate the CO₂ adsorption and dissociation pathways under different oxygen coverage on the Mo₂C catalyst surface. We unravel how the catalyst electronic properties are modified with respect to the presence of surface oxygen and, in turn, how this electronic modification impacts the elementary steps of CO₂ reduction to CO. Importantly, our computational results explain the experimentally observed, selective CO₂ conversion to CO on pristine and K-promoted Mo₂C catalysts.

Computational Methods

DFT calculations were performed using the Vienna *ab initio* simulation package (VASP).³⁵ The Perdew–Burke–Ernzerhof (PBE) exchange-correlation functional was employed within the generalized gradient approximation (GGA).³⁶ The crystal structure of β-Mo₂C has an orthorhombic ground state structure with the space group (*Pbcn*) and lattice parameters of *a* = 5.195 Å, *b* = 6.022 Å, and *c* = 4.725 Å.³⁷ By applying geometry optimizations based on minimization of the total energy of the unit cell, the DFT lattice parameters are obtained to be *a* = 5.250 Å, *b* = 6.071 Å, and *c* = 4.749 Å, which are in good agreement with the experimentally obtained ones. For all the studies pertinent to β-Mo₂C (001) surface, a (2 × 2) supercell was employed. Previously, it was found that CO₂ does not chemisorb on the C-terminated β-Mo₂C (001) surface.³³ Therefore, Mo-terminated Mo₂C (001) surface was considered

in this study. The supercell of the slab model has 32 atoms of molybdenum (Mo), and 16 atoms of carbon (C), with a cell dimension of 12.15 Å × 10.50 Å × 14.55 Å. The vacuum space was set to 10 Å in all calculations. For K-promoted β-Mo₂C (001), one K atom was placed at different sites of the top layer of the carbide, and after geometry optimization, the site that exhibited the strongest binding to K atom was selected for further calculations (K-promoted β-Mo₂C (001) surface). To study the effect of oxygen coverage, several possible oxygen binding sites were considered to identify the most energetically preferred adsorption sites. Including the clean surface (0 ML coverage), five different oxygen coverages were investigated, namely, 0.25 ML, 0.50 ML, 0.75 ML, 1.00 ML, and 1.25 ML, and the CO₂ adsorption behavior on these systems was studied. The kinetic energy cutoff was set to 415 eV,¹⁵ the convergence criteria to 10⁻⁶ eV for the total electronic energy and 0.01 eV Å⁻¹ for the forces acting on atoms. The *k*-point mesh was a 5 × 5 × 1 *k*-point grid generated by Monkhorst–Pack scheme.³⁸ The climbing image-nudged elastic band (CI-NEB) method³⁹ was applied to locate transition states in the CO₂ dissociation pathway. During geometry optimizations, the bottom two layers were fixed in their bulk positions, whereas all the other atoms were allowed to relax. Vibrational frequencies on the adsorbates were performed to verify local minima and transition states (presence of one imaginary mode).

The binding energy (BE) is calculated as:

$$\text{BE}_{(\text{adsorbate})} = E_{(\text{surface+adsorbate})} - E_{(\text{surface})} - E_{(\text{adsorbate})} \quad (3)$$

where *E*_(surface+adsorbate) is the total electronic energy of the surface with the adsorbed CO₂, *E*_(surface) is the corresponding energy of the clean surface (without any adsorbate), and *E*_(adsorbate) is that of the CO₂ molecule. To examine the charge transfer, the difference charge density (DCD) was computed, which is defined as:

$$\rho_{\text{diff}} = \rho_{\text{CO}_2;\text{Surface}} - \{\rho_{\text{Surface}} + \rho_{\text{CO}_2}\} \quad (4)$$

where ρ_{diff} is the DCD, $\rho_{\text{CO}_2;\text{Surface}}$ is the charge density of system with CO₂ adsorbed on the surface. ρ_{Surface} and ρ_{CO_2} are the charge densities of corresponding surface and CO₂, respectively. To compute the DCD, the catalyst surface and CO₂ were kept fixed to the corresponding optimized positions of the chemisorbed state (CO₂:surface).

The d-band center (ε_d^c) was used to correlate the catalytic properties with the electronic structure of the catalyst. It is qualitatively defined as the average energy of the d-states of a catalyst and it was calculated as:

$$\varepsilon_d^c = \frac{\int_{-10}^{E_F} \varepsilon n(\varepsilon) d\varepsilon}{\int_{-10}^{E_F} n(\varepsilon) d\varepsilon} \quad (5)$$

where $n(\varepsilon)$ represents the density of states projected onto d-states and we integrated over occupied states of the metals (Mo).

Results and discussion

The nature of interaction between CO₂ and Mo₂C surfaces

Previous theoretical calculations showed noticeable enhancement in the BEs of CO₂ on Mo₂C with K-promotion ($-46.4 \text{ kcal mol}^{-1}$) compared to that on clean Mo₂C ($-31.4 \text{ kcal mol}^{-1}$).³³ Initially, we examine the adsorption strength of K on the Mo₂C surface. The calculated BEs show that K prefers to adsorb on the hollow site (BE = $-52.5 \text{ kcal mol}^{-1}$) over the top site (BE = $-46.5 \text{ kcal mol}^{-1}$). In order to understand the enhancement in CO₂ BE on K-promotion, we performed DCD analysis. DCDs of clean and K-promoted Mo₂C are shown in Fig. 1. Positive DCD (red) shows charge loss (holes) and negative DCD (green) shows charge gain (electrons). DCD analysis suggests that the activation of CO₂ involves charge gain from the surface through both the carbon and oxygen atoms. The size lobes of DCD is also found to be enhanced with K promotion, indicating an increased charge gain.

The computed net (Bader) charges on the activated state of CO₂ at clean and K promoted surface were found to be -1.21 e and -1.42 e , respectively. The increase in the Bader charge of CO₂ also indicates enhanced charge transfer with K promotion. Above analysis suggests that the interaction of CO₂ with Mo₂C surface involves charge transfer from the surface to CO₂, and K-promotion increases the charge transfer, thereby increasing the CO₂ BE.

Effect of oxygen coverage of Mo₂C surface on CO₂ adsorption

Previous studies suggested that under experimental conditions the metal carbide surface may be converted to an oxygenated carbide surface.^{9,33,40} To investigate the effect of oxygenation of Mo₂C surface on CO₂ adsorption, we calculated the oxygen BE under five different surface coverages ranging from 0.25 ML (monolayer) to 1.25 ML, as shown in Fig. 2. The BE of oxygen was calculated by eqn (6):

$$E(O) = E(nO\text{-surf}) - nE(H_2) - nE(H_2O) \quad (6)$$

where n is the number of oxygen atoms adsorbed in one supercell. Because of the complex electronic structure of O₂ molecule, DFT calculations with GGA functionals have the tendency to underestimate the oxygen BEs.⁴¹ As a result, in the computation of oxygen BEs, water is often used as a reference,⁴² as demonstrated in eqn (5). The optimized O-covered Mo₂C (001) surface are shown in Fig. 2. The most preferred adsorption site for the oxygen atoms was found to be the hollow site. At one ML O-coverage, all of the hollow sites are found to be occupied by oxygen, and therefore further addition of oxygen atoms to the surface is expected to be endothermic. From Fig. 3, one can observe that the total BE of oxygen increases (more exothermic) as the O-coverage increases up to 1 ML. This trend was found to be altered (decrease in BE) when the surface O-coverage was further increased from 1 ML to 1.25 ML.

Binding of CO₂ and CO on oxygen covered Mo₂C surfaces

The most preferential site for CO₂ chemisorption on the clean β -Mo₂C (001) surface was found to be the hollow site.³³ It is therefore interesting to investigate how CO₂ adsorption behavior changes with surface O-coverage under reaction conditions, as O preferentially binds to these hollow sites. Therefore, different sites must be investigated in order to obtain the most stable chemisorption configuration of CO₂. On 0.25 ML O-coverage, three different sites (shown in Fig. 4) were found to be capable of activating CO₂, with the strongest BE at the hollow site ($-18.8 \text{ kcal mol}^{-1}$). At this site, the O-C-O bond angle of activated CO₂ was 134.2 degrees, the C-O bond length was 1.27 Å, and the average Mo-O distance was 2.37 Å.

On 0.5 ML O-covered surface, the hollow site was found to activate CO₂ with BE of $-5.37 \text{ kcal mol}^{-1}$, which shows weaker binding compared to that on 0.25 ML ($-18.8 \text{ kcal mol}^{-1}$) and the clean surface ($-29.8 \text{ kcal mol}^{-1}$). The O-C-O bond angle of activated CO₂ was 137.5 degrees, the C-O bond length was 1.25 Å and the average Mo-O length was 2.31 Å. On 0.75 ML O-covered surface, no chemisorption of CO₂ was found, and

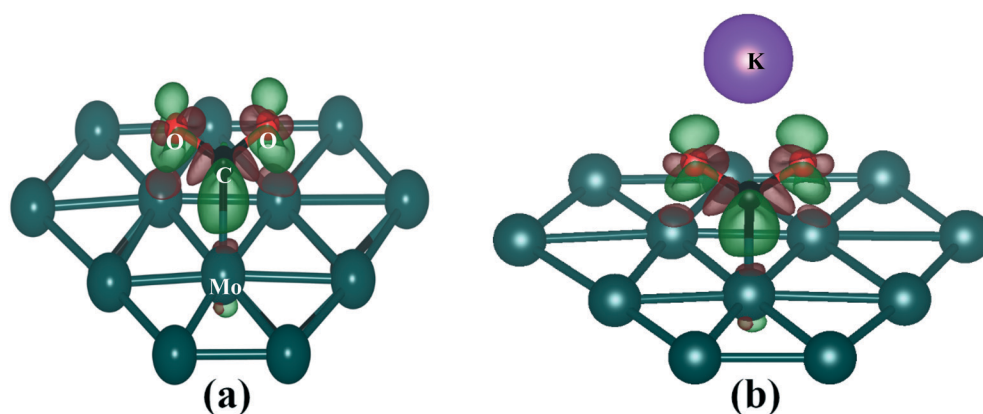


Fig. 1 Difference charge density (with isovalue of $0.01 \text{ e } \text{\AA}^{-3}$) of CO₂ adsorbed on (a) pristine and (b) K-promoted Mo₂C surface. Color codes: Mo-green, carbon-black, oxygen-red and K-purple. Truncated part of the surface is shown for the sake of clarity.

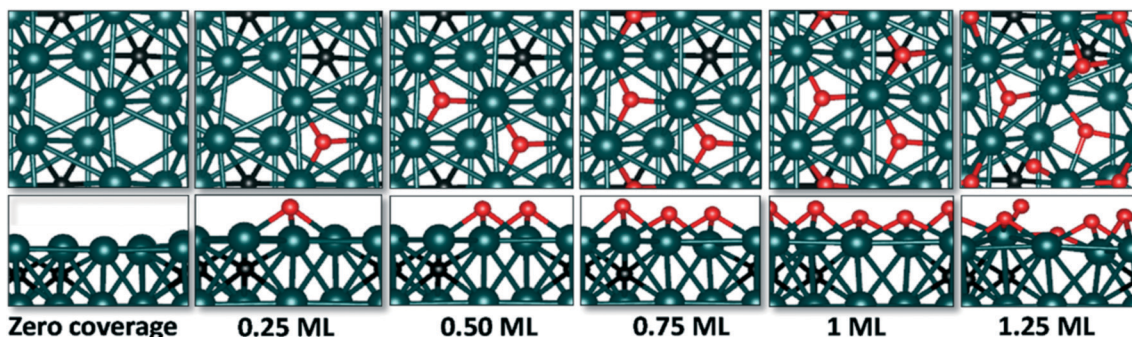


Fig. 2 (From left to right) Optimized O-Mo₂C (001) surfaces at 0.00 ML (clean surface), 0.25 ML, 0.50 ML, 0.75 ML, 1 ML, and 1.25 ML oxygen coverage, with top and side view. Truncated part of the surface is shown for the sake of clarity.

a positive BE of +12.0 kcal mol⁻¹ was calculated, indicating that the interaction of CO₂ becomes endothermic on surfaces with high O-coverage. The activation/adsorption of CO₂ on 0.5 ML and 0.75 ML O-covered surfaces are shown in Fig. 5.

Fig. 6 summarizes the BE of CO₂ vs. O-coverage. It can be observed that the BE of CO₂ follows a linear trend: the lower the O-coverage, the stronger the CO₂ adsorption (larger negative BE (CO₂) values). However, at O-coverage larger than 0.75 ML, the interaction of CO₂ with the surface becomes endothermic, and the adsorption of CO₂ is no longer favorable.

CO₂ dissociation barriers on oxygen covered surfaces

To calculate the activation energy for CO₂ dissociation, CI-NEB calculations were carried out. Several CO₂ dissociated (CO* + O*) configurations were constructed by placing the CO* at a particular site, and varying the location of O* at neighboring sites and minimizing the total energies of the different configurations. After obtaining the most stable dissociated configuration, this structure was considered as the final state (dissociated CO₂) for CI-NEB calculations, and the corresponding reaction path was then constructed. The activation barriers for CO₂ dissociation on 0.25 ML and 0.50 ML

O-Mo₂C surfaces were found to be 23.57 kcal mol⁻¹ and 26.89 kcal mol⁻¹, respectively. The distances of O-CO bond of the transition states were found to be 1.750 Å (0.25 ML) and 1.753 Å (0.50 ML).

In Fig. 7 we show the activation energy profiles of CO₂ dissociation on (1) pristine surface, (2) K-promoted, (3) 0.25 ML O-covered, (4) 0.50 ML O-covered, and (5) K-promoted 0.25 ML O-covered Mo₂C (001) surface. Interestingly, we found that while the presence of a surface K atom decreases the activation energy of CO₂ dissociation, the surface O atoms increase the CO₂ dissociation barrier. Visual inspection of Fig. 7 suggests that the transition state for CO₂ dissociation is an early (reactant-like) transition state. Therefore, for CO₂ dissociation the stabilization of initial state should also stabilize the transition state, resulting in lowering the activation barriers. Consequently, one would expect that higher CO₂ BE (stabilization of TS) would result in lower activation energies for CO₂ dissociation. Indeed, we note a linear correlation (Fig. S1,† the weaker the CO₂ binding, the higher the CO₂ dissociation barrier) between the CO₂ BE and the calculated activation barriers for CO₂ dissociation under different O-coverage. As shown previously, the surface K atom acts as an electron donor, facilitates the charge transfer to CO₂ and enhances adsorption of CO₂. Oxygen atoms, however, occupy the preferred sites for CO₂ adsorption, form an oxy-molybdate surface, which introduces repulsion to the adsorbents containing oxygen (*i.e.* CO₂), and consequently decrease the adsorption of CO₂ on the surface. For the conversion of CO₂ using RWGSR, the product (CO) must be desorbed from the surface. As noted previously,³³ the desorption energies of CO, from the dissociated state of CO₂ (CO* + O*), are highly endothermic on clean (and K promoted) Mo₂C. Interestingly, we note that CO desorption energies decrease with oxygen coverage (Table 1), indicating an important role of oxygen coverage in the desorption of the product.

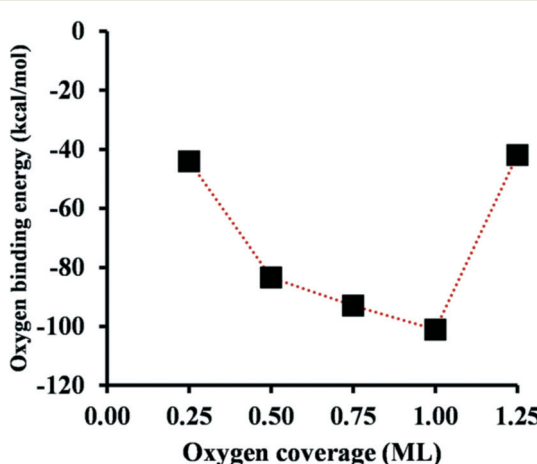


Fig. 3 BE of oxygen at coverages ranging from 0.25 ML to 1.25 ML (Mo-terminated Mo₂C).

Electronic structure

We further investigated the electronic structure of Mo₂C catalyst as a function of oxygen coverage. Fig. 8 displays the projected density of states (PDOS) of Mo atoms involved in CO₂ bonding. Total density of states (DOS) in Fig. S2,†

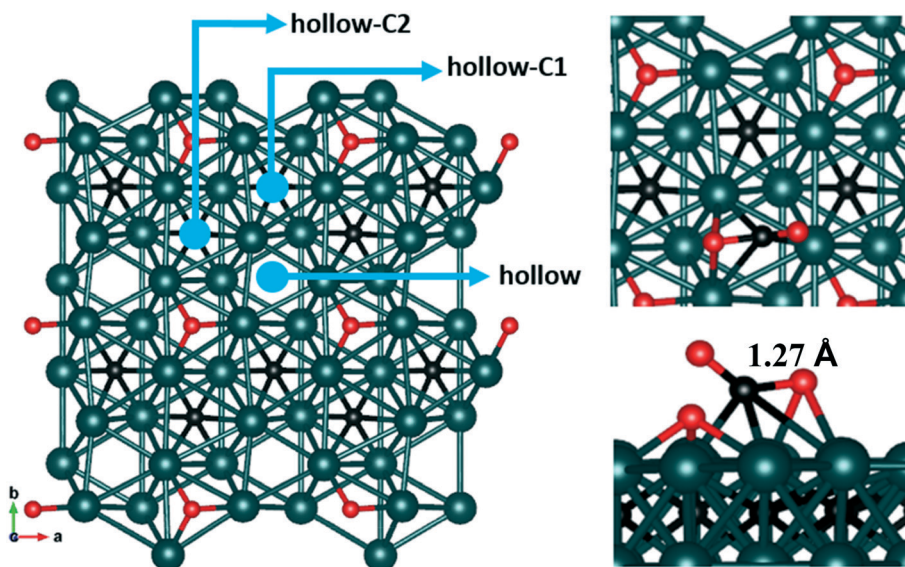


Fig. 4 (left) Top view of 0.25 ML O-covered Mo_2C (001), with three different adsorption sites pointed in blue. (right) CO_2 adsorption on 0.25 ML O- Mo_2C (001) surface at hollow site from top and side view.

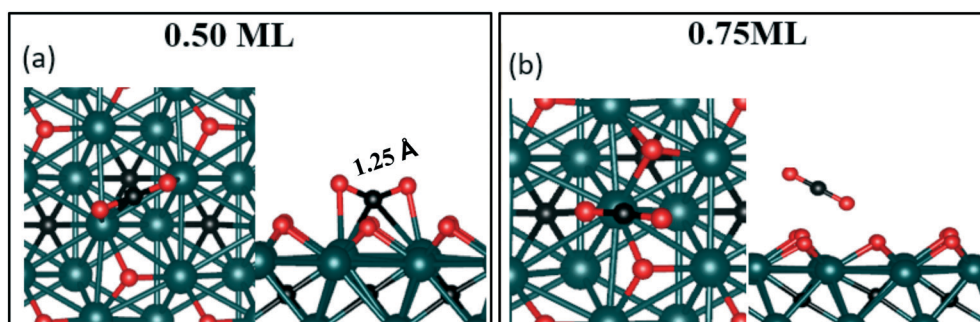


Fig. 5 CO_2 adsorption on (a) 0.50 ML and (b) 0.75 ML of O-covered Mo_2C (001) in top and side view.

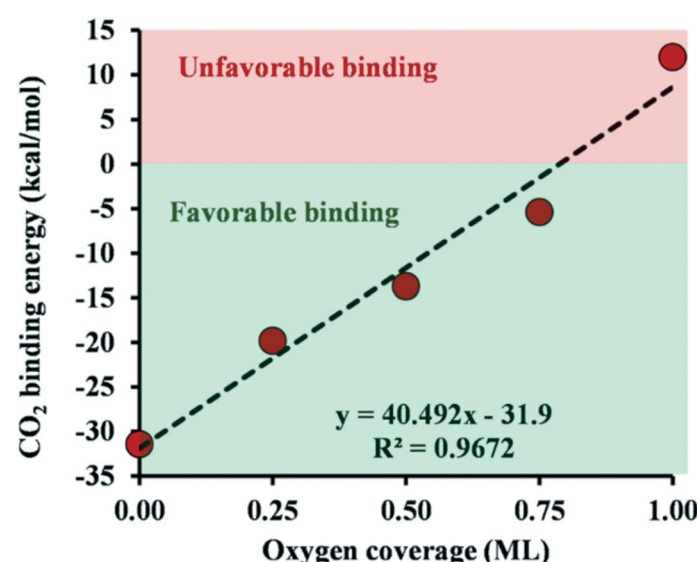


Fig. 6 BE of CO_2 vs. oxygen coverage on Mo_2C (001) surface (the most preferred binding sites on each O-coverage surface).

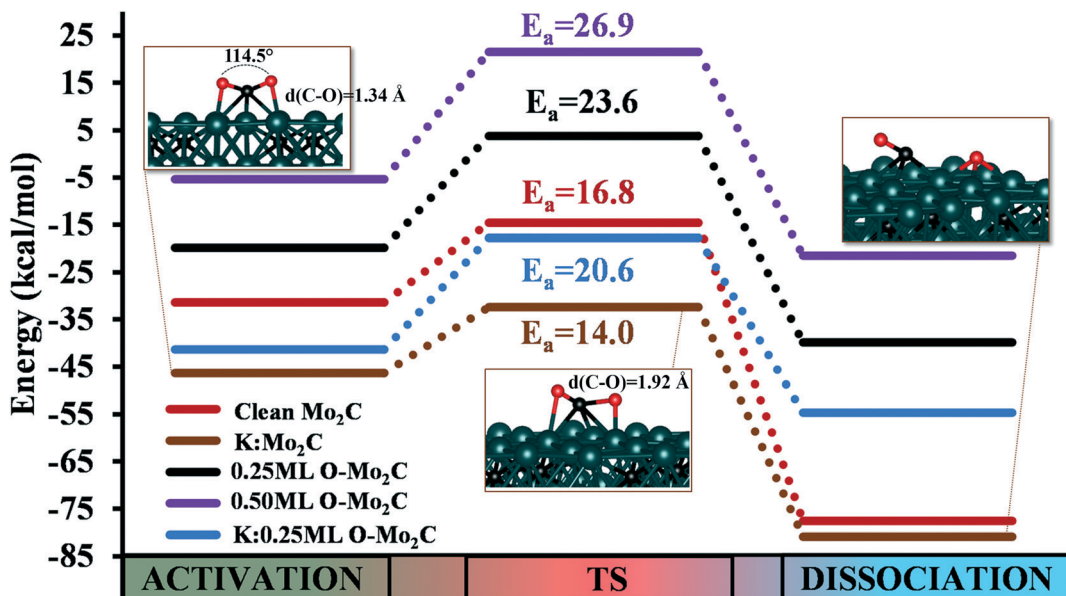


Fig. 7 CO_2 dissociation profiles on pristine (red), 0.25 ML O-covered (black), 0.50 ML O-covered (purple), K-doped (brown) and K-doped 0.25 ML O-covered (blue) surfaces. E_a represents activation energy in kcal mol^{-1} .

demonstrate that even with oxygen coverage Mo_2C shows metallic character. Previous studies demonstrated that the activation of CO_2 requires electron transfer from the catalyst to CO_2 .^{43–46} The electron donation capacity of any catalyst can be determined based on the electronic population near the Fermi level. Interestingly, DOS analysis suggests that the electronic population near Fermi level decreases with oxygen coverage. To quantify the electronic occupation of Mo atoms near Fermi level, we integrated the PDOS in the range of -2.0 eV to 0.0 eV (E_{Fermi}). Fig. 9(a) demonstrates the d-occupation of Mo atoms (responsible for CO_2 activation). Notably, the Mo d-occupation decreases with the increase in the oxygen coverage, suggesting that the number of electrons available on Mo near the Fermi level decreases.

Based on this decrease of the electronic occupancy near the Fermi level, one would expect the electron transfer from Mo_2C to CO_2 to decrease with oxygen coverage. Consequently, the BE of CO_2 on Mo_2C are expected to decrease with oxygen coverage, in agreement with our results presented in Fig. 6. The change in the electronic structure of Mo_2C due to oxygen coverage also weakens the strong interaction between CO^* and the surface. The CO desorption energies are also found to decrease with increasing oxygen coverage (Table 1). More-

over, with increasing oxygen coverage, the further dissociation of $\text{CO}^* \rightarrow \text{C}^* + \text{O}^*$ is not favored, both kinetically and thermodynamically (Fig. S3a†), demonstrating an inverse relationship between CO desorption and dissociation⁴⁷ (Fig. S3b†).

In addition to the d-occupation near the Fermi level, we calculated the d-band center⁴⁸ of occupied states of Mo atoms under different O-coverage (Fig. 9(b)). The occupied d-band center was calculated due to the increase in the charge transfer from the occupied states of Mo to the surface-bound oxygen atoms with oxygen coverage. The occupied d-band center corresponds to the center of bonding d-states of Mo near the Fermi level and with the decrease in the occupancies of the states near the Fermi level (charge transfer from highest occupied bands), the d-band center shifts to lower energies. We found that as the O-coverage increases, the Mo d-band center moves away from the Fermi level, decreasing the adsorption of CO_2 . Fig. S4 and S5† show the correlation of CO_2 BEs with d-band center and with the occupation of d-states near Fermi level, respectively. We note that the d-band center and the occupation of d-states near Fermi level could be used as interchangeable descriptors for CO_2 BEs on Mo_2C .

The analysis of CO_2 adsorption, CO desorption and the electronic structure of Mo_2C suggest that oxygen coverage determines the strength of interaction of the adsorbates with the catalyst. At low O-coverage both CO_2 and CO bind strongly to the surface and with an increase in oxygen coverage the strength of this interaction decreases. As noted previously by Porosoff *et al.*, CO binds too strongly with clean Mo_2C .³³ However, the presence of surface oxygen (forming oxy-molycarbide) is important in tuning the CO desorption from the surface.

Table 1 Desorption energy of CO with oxygen coverage on Mo_2C (001) surface

System	Desorption energy (kcal mol ⁻¹)
Clean Mo_2C	51.0
K-doped Mo_2C	51.1
0.25 ML Mo_2C	44.9
0.50 ML Mo_2C	28.8
K-doped 0.25 ML Mo_2C	50.7

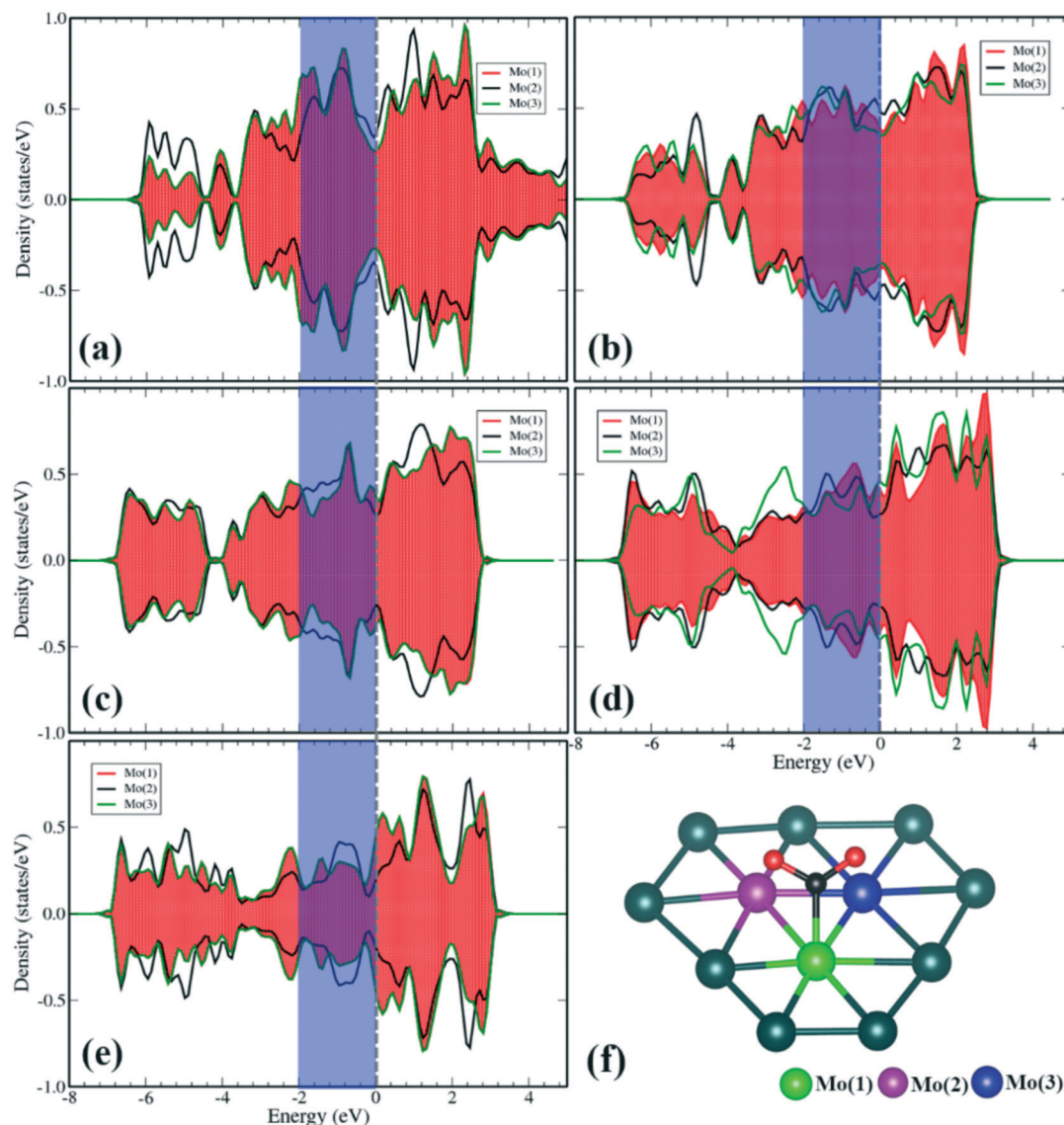


Fig. 8 Projected density of states (PDOS) of (a) pristine Mo_2C , and Mo_2C with oxygen coverage of (b) 0.25 ML, (c) 0.50 ML, (d) 0.75 ML, (e) 1.0 ML. (f) Activated state of CO_2 over in pristine Mo_2C .

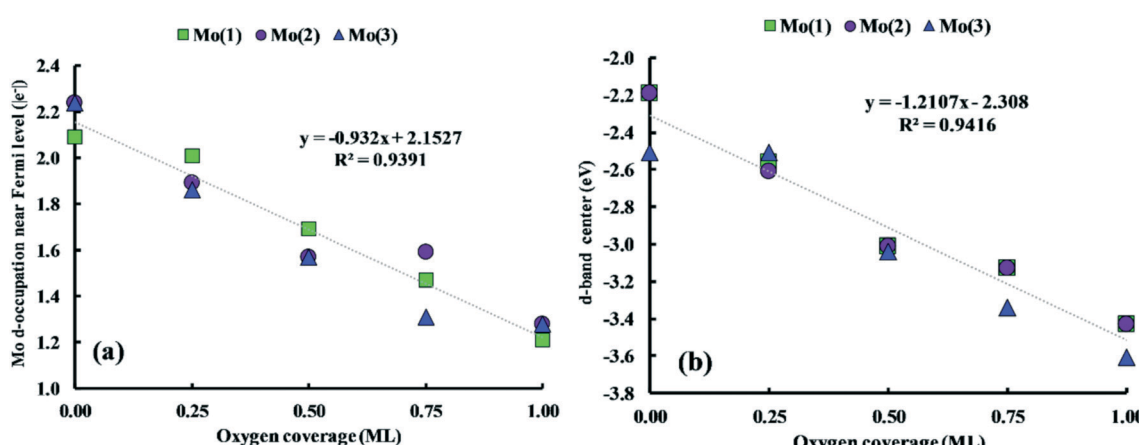


Fig. 9 (a) Occupation of d-states near Fermi level and (b) d-band center of Mo atoms at different oxygen coverage.

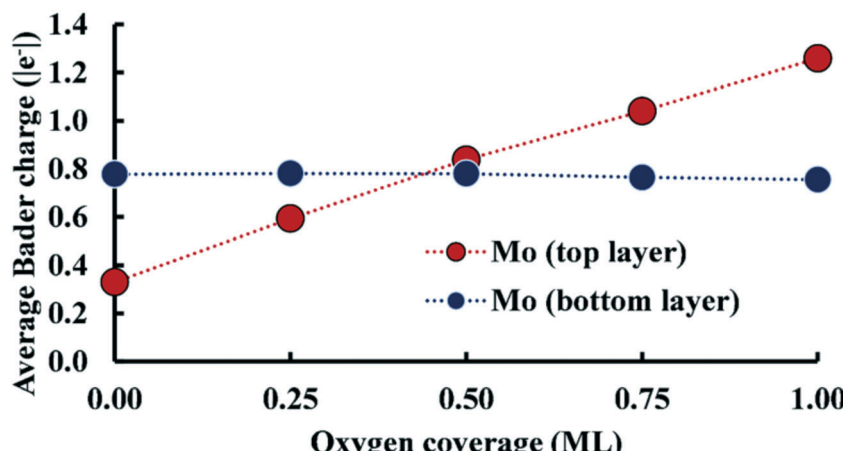


Fig. 10 Average Bader charges on Mo atoms in top and bottom layers in Mo_2C with different oxygen coverage.

Bader charge of Mo atoms with oxygen coverage

We employed Bader charge analysis to further solidify our conclusions regarding the reduction in the electronic population of Mo atoms in Mo_2C with oxygen coverage. The average Bader charges of the top and bottom layer Mo atoms are given in Fig. 10 while charges on other atoms are given in Table S1.[†] We observe a linear increase in the positive charge (electron loss) with oxygen coverage, indicating an increased Mo to oxygen electron transfer with oxygen coverage. Since the oxygen atoms were adsorbed on the surface, the change in the charge was noticed primarily on surface atoms, whereas the charge on Mo atoms in bottom layer was found to be almost constant with increasing the oxygen coverage (Fig. 10). Interestingly, Porosoff *et al.* observed that Mo in Mo_2C exists in different oxidation states (Mo^{2+} , Mo^{3+} , Mo^{4+} , Mo^{5+} , and Mo^{6+}). The authors demonstrated that the high oxidation (Mo^{3+} and Mo^{5+}) states of Mo correspond to oxy-molycarbide whereas the low oxidation state of Mo (Mo^{2+}) corresponds to clean molycarbide.³³ In line with these experimental findings, the increase in positive Bader charge of surface Mo atoms indicates the change in their formal oxidation states due to oxygen adsorption (formation of oxy-molycarbide).

Conclusions

The adsorption and dissociation behavior of CO_2 on $\beta\text{-Mo}_2\text{C}$ (001) was investigated as a function of oxygen coverage on the catalyst surface using DFT calculations and electronic structure analysis. According to our results, the activation of CO_2 on Mo_2C involves charge donation from the surface to CO_2 through both carbon and oxygen atoms. The total (absolute) binding energy of oxygen on the Mo_2C surface increases as the surface O-coverage increases, until it reaches a maximum at 1 ML coverage. CO_2 binding energy decreases with the increase in surface oxygen atoms and CO_2 can no longer chemisorb at high oxygen coverage (O-coverage > 0.5 ML). The high exothermicity of dissociated state of CO_2 (CO^* and O^*) is found to be significantly reduced with oxygen coverage,

and CO desorption energies decrease with increasing oxygen coverage. Finally, it should be noted that even though the Mo_2C surface can become an oxy- Mo_2C surface under reaction conditions, our study shows that CO_2 can still adsorb and dissociate at low O-coverage (< 0.50 ML). Our results rationalize a series of previously reported experimental observations.^{9,32,33}

Conflicts of interest

There are no conflicts of interest to declare.

Acknowledgements

This work was supported by the U.S. Naval Research Laboratory (NRL) and in part by the University of Pittsburgh Center for Research Computing through the resources provided.

References

- M. Mikkelsen, M. Jorgensen and F. C. Krebs, *Energy Environ. Sci.*, 2010, 3, 43–81.
- D. M. D'Alessandro, B. Smit and J. R. Long, *Angew. Chem., Int. Ed.*, 2010, 49, 6058–6082.
- D. A. Lashof and D. R. Ahuja, *Nature*, 1990, 344, 529–531.
- R. Mendelsohn, W. D. Nordhaus and D. Shaw, *Am. Econ. Rev.*, 1994, 84, 753–771.
- R. Socolow, M. Desmond, R. Aines, J. Blackstock, O. Bolland, T. Kaarsberg, N. Lewis, M. Mazzotti, A. Pfeffer, K. Sawyer, J. Siiriola, B. Smit and J. Wilcox, *Direct Air Capture of CO₂ with Chemicals: A Technology Assessment for the APS Panel on Public Affairs*, American Physical Society, 2011.
- C. Song, *Catal. Today*, 2006, 115, 2–32.
- W. Wang, S. Wang, X. Ma and J. Gong, *Chem. Soc. Rev.*, 2011, 40, 3703–3727.
- M. Mikkelsen, M. Jørgensen and F. C. Krebs, *Energy Environ. Sci.*, 2010, 3, 43–81.
- M. D. Porosoff, X. Yang, J. A. Boscoboinik and J. G. Chen, *Angew. Chem., Int. Ed.*, 2014, 53, 6705–6709.
- H. Shou and R. J. Davis, *J. Catal.*, 2011, 282, 83–93.

- Published on 10 October 2017. Downloaded by Indian Institute of Science Education & Research Kolkata on 7/23/2020 5:23:24 PM.
- 11 R. W. Dorner, D. R. Hardy, F. W. Williams, B. H. Davis and H. D. Willauer, *Energy Fuels*, 2009, **23**, 4190–4195.
 - 12 E. Iglesia, *Appl. Catal., A*, 1997, **161**, 59–78.
 - 13 R. Levy and M. Boudart, *Science*, 1973, **181**, 547–549.
 - 14 S. T. Oyama, in *The Chemistry of Transition Metal Carbides and Nitrides*, ed. S. T. Oyama, Springer Netherlands, Dordrecht, 1996, pp. 1–27.
 - 15 S. Posada-Perez, F. Vines, P. J. Ramirez, A. B. Vidal, J. A. Rodriguez and F. Illas, *Phys. Chem. Chem. Phys.*, 2014, **16**, 14912–14921.
 - 16 J. B. Claridge, A. P. E. York, A. J. Brungs, C. Marquez-Alvarez, J. Sloan, S. C. Tsang and M. L. H. Green, *J. Catal.*, 1998, **180**, 85–100.
 - 17 E. Furimsky, *Appl. Catal., A*, 2003, **240**, 1–28.
 - 18 S. T. Oyama, J. C. Schlatter, J. E. Metcalfe and J. M. Lambert, *Ind. Eng. Chem. Res.*, 1988, **27**, 1639–1648.
 - 19 S. Ramanathan and S. T. Oyama, *J. Phys. Chem.*, 1995, **99**, 16365–16372.
 - 20 M. Nagai and K. Matsuda, *J. Catal.*, 2006, **238**, 489–496.
 - 21 J. A. Schaidle, A. C. Lausche and L. T. Thompson, *J. Catal.*, 2010, **272**, 235–245.
 - 22 R. Barthos and F. Solymosi, *J. Catal.*, 2007, **249**, 289–299.
 - 23 J. S. Lee, S. Locatelli, S. Oyama and M. Boudart, *J. Catal.*, 1990, **125**, 157–170.
 - 24 F. Solymosi, R. Németh, L. Óvári and L. Egri, *J. Catal.*, 2000, **195**, 316–325.
 - 25 S. Posada-Pérez, F. Viñes, J. A. Rodriguez and F. Illas, *Top. Catal.*, 2014, **58**, 159–173.
 - 26 J. A. Rodriguez, P. Liu, D. J. Stacchiola, S. D. Senanayake, M. G. White and J. G. Chen, *ACS Catal.*, 2015, **5**, 6696–6706.
 - 27 J. J. Mortensen, B. Hammer and J. K. Nørskov, *Phys. Rev. Lett.*, 1998, **80**, 4333–4336.
 - 28 S. Linic and M. A. Barateau, *J. Am. Chem. Soc.*, 2004, **126**, 8086–8087.
 - 29 H. Xin and S. Linic, *J. Chem. Phys.*, 2016, **144**, 234704.
 - 30 J. S. Lee, S. Kim and Y. G. Kim, *Top. Catal.*, 1995, **2**, 127–140.
 - 31 L. Bugyi and F. Solymosi, *J. Phys. Chem. B*, 2001, **105**, 4337–4342.
 - 32 F. Solymosi and L. Bugyi, *Catal. Lett.*, 2000, **66**, 227–230.
 - 33 M. D. Porosoff, J. W. Baldwin, X. Peng, G. Mpourmpakis and H. D. Willauer, *ChemSusChem*, 2017, **10**, 2408–2415.
 - 34 M. Marwood, R. Doepper and A. Renken, *Appl. Catal., A*, 1997, **151**, 223–246.
 - 35 G. Kresse and J. Furthmüller, *Comput. Mater. Sci.*, 1996, **6**, 15–50.
 - 36 J. P. Perdew, K. Burke and M. Ernzerho, *Phys. Rev. Lett.*, 1996, **77**, 3865–3868.
 - 37 E. Parthe and V. Sadogopan, *Acta Crystallogr.*, 1963, **16**, 202–205.
 - 38 J. D. Pack and H. J. Monkhorst, *Phys. Rev. B: Solid State*, 1977, **16**, 1748–1749.
 - 39 D. Sheppard, R. Terrell and G. Henkelman, *J. Chem. Phys.*, 2008, **128**, 134106.
 - 40 P. Liu and J. A. Rodriguez, *J. Phys. Chem. B*, 2006, **110**, 19418–19425.
 - 41 L. Wang, T. Maxisch and G. Ceder, *Phys. Rev. B: Condens. Matter Mater. Phys.*, 2006, **73**, 195107.
 - 42 J. Rossmeisl, A. Logadottir and J. K. Nørskov, *Chem. Phys.*, 2005, **319**, 178–184.
 - 43 N. Austin, J. Ye and G. Mpourmpakis, *Catal. Sci. Technol.*, 2017, **7**, 2245–2251.
 - 44 H.-J. Freund and M. W. Roberts, *Surf. Sci. Rep.*, 1996, **25**, 225–273.
 - 45 W. Wurth, J. Stöhr, P. Feulner, X. Pan, K. Bauchspies, Y. Baba, E. Hudel, G. Rocker and D. Menzel, *Phys. Rev. Lett.*, 1990, **65**, 2426.
 - 46 N. Austin, B. Butina and G. Mpourmpakis, *Prog. Nat. Sci.: Mater. Int.*, 2016, **26**, 487–492.
 - 47 X. Chen, X. Su, H.-Y. Su, X. Liu, S. Miao, Y. Zhao, K. Sun, Y. Huang and T. Zhang, *ACS Catal.*, 2017, **7**, 4613–4620.
 - 48 B. Hammer and J. Nørskov, *Surf. Sci.*, 1995, **343**, 211–220.